

## INTERBAND BREAKDOWN AND THE PINCH EFFECT IN BISMUTH-ANTIMONY ALLOYS

N. B. BRANDT, E. A. SVISTOV, E. A. SVISTOVA, and G. D. YAKOVLEV

Moscow State University

Submitted March 15, 1971

Zh. Eksp. Teor. Fiz. 61, 1078-1086 (September, 1971)

The current-voltage characteristics of  $\text{Bi}_{1-x}\text{Sb}_x$  ( $x = 0.065 - 0.22$ ) semiconducting alloys are studied in electric fields up to 30 V/cm at temperatures between 2 and 20°K. The effect of magnetic fields (up to 200 Oe) on their shape is also studied. The results indicate that the following effects arise in strong electric fields: 1) Interband breakdown, which is observed at electric field strengths varying between 1 and 14 V/cm, depending on the Sb concentration. 2) Decrease of mobility in pre-breakdown fields, due to heating of the carrier gas by the strong electric field and to alteration of the nature of their scattering. 3) The pinch effect in an electron-hole plasma produced as a result of interband breakdown.

## INTRODUCTION

THE study of the properties of the semiconducting single-crystal alloys  $\text{Bi}_{1-x}\text{Sb}_x$  ( $x = 0.065-0.22$ ) in strong electric fields is of great interest, owing to the small forbidden band, which can range from 0 to 24 MeV when the antimony concentration is varied<sup>[1]</sup>. In the antimony-concentration interval  $x \sim 0.065-0.085$ , the minimum energy gap is determined by the extrema  $L_S$  and  $T_{45}$ , which are located at the points L and T of the Brillouin zone; in the interval 0.085-0.17 it is determined by the extrema  $L_A$  and  $L_S$ , located in the same point of phase space, and at  $x > 0.17$  it is determined by the extrema  $L_A$  and  $T_6$  (see Fig. 1 of<sup>[1]</sup>).

The high mobilities ( $\sim 10^6$  cm<sup>2</sup>/V-sec at  $T = 4.2^\circ\text{K}$ )<sup>[2]</sup> make it possible to observe already in fields on the order of several V/cm effects connected with heating of the carrier gas, such as the change of mobility with the changing field, the alteration of the predominant scattering mechanism, and interband breakdown. (We note that owing to the large lattice dielectric constant  $\kappa = 100$  and the small effective carrier masses  $m^* \approx 0.01 m_0$ , all the impurities in these materials are thermally ionized already at helium temperatures.)

The occurrence of a compensated electron-hole plasma in  $\text{Bi}_{1-x}\text{Sb}_x$  samples as a result of interband breakdown uncovers, in turn, the possibility of investigating certain pure plasma effects, such as the pinch effect, plasma instabilities, etc.

In<sup>[3]</sup>, using strongly doped  $\text{Bi}_{0.88}\text{Sb}_{0.12}$  alloys in electric fields on the order of  $\sim 10$  V/cm at  $T = 4.2^\circ\text{K}$ , an increase of the conductivity was observed, apparently connected with the occurrence of interband breakdown. A similar phenomenon was also observed in pure  $\text{Bi}_{1-x}\text{Sb}_x$  single crystals<sup>[4]</sup>.

We report here the results of detailed investigations of the current-voltage characteristics (CVC) of semiconducting single-crystal  $\text{Bi}_{1-x}\text{Sb}_x$  alloys ( $x = 0.065-0.22$ ) at  $4.2^\circ\text{K}$  in electric fields up to 30 V/cm and magnetic fields up to 200 Oe. The experimental data obtained indicate that the main cause of the increase of the conductivity of the samples in fields with intensities of several V/cm is interband breakdown. The

results of the experiments give grounds for assuming that in the pre-breakdown region the character of the carrier scattering changes from predominant scattering by ionized impurities in weak fields to predominant scattering by acoustic phonons. In the post-breakdown region, a pinch effect was observed in the electron-hole plasma produced following interband breakdown.

## SAMPLES. MEASUREMENT PROCEDURE

The samples were cut by the electric-spark method from single-crystal ingots of  $\text{Bi}_{1-x}\text{Sb}_x$  alloys with components better than 99.9999% pure, prepared at the Leningrad State Polytechnic Institute in the laboratory of G. A. Ivanov, and shaped in the form of parallel-epipeds or "dumbbells" (Fig. 1). The sides of the samples coincided, in all combinations, with the principal crystallographic axes: binary  $C_1$ , bisector  $C_2$ , and trigonal  $C_3$ . The cross-section areas of the central part ranged from  $\sim 10^{-3}$  to  $6 \times 10^{-2}$  cm<sup>2</sup>, and the length from  $\sim 0.17$  to  $\sim 0.6$  cm. The samples were etched in concentrated nitric acid, after which they were washed many times with distilled water. The current electrodes were strips of copper foil  $\sim 40$   $\mu$  thick, soldered to the ends of the sample with Wood's alloy (with all precautions to prevent overheating). The potential contacts were copper wires of  $\approx 20$  diameter, welded to the side faces by the electric-spark method<sup>[5]</sup>.

The relative perfection of the  $\text{Bi}_{1-x}\text{Sb}_x$  single crystals for samples with identical antimony concentration was estimated from the ratio  $\delta = \rho(4.2^\circ\text{K})/\rho(300^\circ\text{K})$  of the resistances of the sample at 4.2 and 300°K<sup>[6]</sup>. The parameters of the investigated samples are listed in the table.

Measurements of the CVC and of the Hall emf were performed in a pulsed regime. The current source

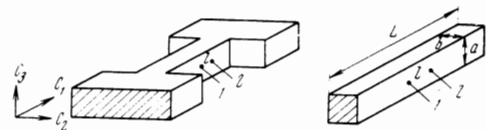


FIG. 1. Shapes of investigated samples: 1, 2—potential contacts. The planes of the current contacts are shown shaded.

Sample number*	Sb concentration, x	Direction of current i	S, 10 <sup>-4</sup> cm <sup>2</sup>	a × b, cm	L, cm	l, cm	δ
1	0.094	C <sub>1</sub>	49	0.057×0.0855	0.35	0.16	1880
2	0.094	C <sub>1</sub>	13	0.057×0.0228	0.33	0.165	2200
3	0.085	C <sub>2</sub>	12	0.035×0.035	0.18	0.035	330
4	0.088	C <sub>3</sub>	28,2	0.091×0.031	0.21	1.02	200
5	0.088	C <sub>2</sub>	32,6	0.058×0.058	0.56	0.137	120
6	0.085	C <sub>1</sub>	46	0.046×0.1	0.4	0.172	348
7	0.088	C <sub>2</sub>	48	0.0638×0.0767	0.174	0.058	130
8	0.088	C <sub>2</sub>	42/116	0.087×0.0493	0.57	0.145	210
9**	0.088	C <sub>2</sub>	44/134	0.046×0.097	0.57	0.074	454
10**	0.088	C <sub>2</sub>	560	0.22×0.255	0.232	0.081	110
11	0.088	C <sub>2</sub>	20,7	0.0464×0.0464	0.56	0.046	190
12	0.088	C <sub>1</sub>	27	0.06×0.045	0.46	0.085	295
13	0.088	C <sub>3</sub>	32	0.0696×0.0464	0.25	0.0407	—
14	0.088	C <sub>2</sub>	64	0.087×0.069	0.17	0.058	150
15	0.088	C <sub>1</sub>	32	0.058×0.052	0.17	0.058	—
16	0.094	C <sub>2</sub>	50	0.068×0.074	0.33	0.103	—
17	0.18	C <sub>1</sub>	62	0.057×0.108	-0.33	0.071	21
18	0.2	C <sub>1</sub>	26	0.057×0.0455	-0.3	0.097	3000
19	0.18	C <sub>1</sub>	62	0.091×0.068	-0.33	0.118	25
20	0.085	C <sub>1</sub>	36	0.057×0.063	-0.3	0.102	170
21	0.07	C <sub>1</sub>	40	0.063×0.063	0.3	0.15	22
22	0.072	C <sub>1</sub>	38	0.074×0.051	0.33	0.165	110
23	0.072	C <sub>1</sub>	32,6	0.057×0.057	0.32	0.109	190

\*All samples were of n-type. For samples with x = 0.088, the carrier density was n<sub>0</sub> = 3 × 10<sup>14</sup> cm<sup>-3</sup>.

\*\*Samples with dumbbell shape. The areas of the current contacts and of the cross section in the central part are indicated.

was a thyatron oscillator with a discharge line, making it possible to obtain rectangular current pulses up to 350 A, duration 2–20 μ sec, and repetition frequency 1 Hz. The output resistance of the generator was in all cases more than 10 times the sample resistance.

The current was supplied to the sample through a coaxial line. The voltage from the potential (or Hall) contacts was fed through coaxial lines to a pulsed oscilloscope (S1-17) with a differential input amplifier. The current amplitude was measured by connecting in series with the sample a resistor of known value, the voltage from which was fed to the second input of the same oscilloscope.

The maximum current and pulse duration in each experiment were chosen such that the effects connected with the possible heating of the sample by the current did not exceed the measurement accuracy. The criterion for this was the reproducibility of the results for different pulse lengths, and also the absence of waveform distortion of the voltage pulse on the sample, which is characteristic of heating.

Most measurements were made at T = 4.2°K. The procedure described in<sup>[7]</sup> was used to obtain temperatures in the interval 4.2–20°K.

## MEASUREMENT RESULTS

Figures 2 and 3 show the CVC of single-crystal samples of Bi<sub>1-x</sub>Sb<sub>x</sub> alloys with antimony concentrations x = 0.072 (No. 23), 0.085 (No. 3), 0.088 (No. 4) and 0.20 (No. 18) in the electric-field interval 0.3–30 V/cm<sup>1)</sup>. We see that when the electric field is increased, the conductivity of most samples is first noticeably decreased (by a factor 1.5–2). Then, in still stronger electric fields, the differential conductivity of the samples increases sharply, and for certain samples (Nos. 1–5) the CVC have in this region an

<sup>1)</sup>The results of the investigation of the CVC of the samples at E < 0.3 V/cm will be published in a separate paper.

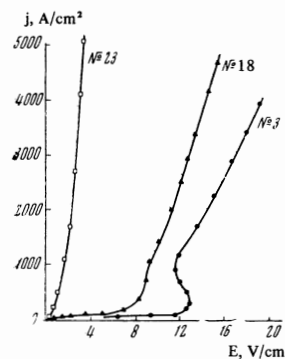


FIG. 2. CVC of a number of samples.

S-shaped form (32), i.e., a section with negative differential conductivity is observed.

The field E<sub>c</sub> at which the sharp increase of the conductivity occurs depends on the quality of the single crystal, the antimony concentration, and the temperature. Samples of relatively lower quality (i.e., with smaller values of δ and carrier mobilities) have larger values of E<sub>c</sub>—see Fig. 4. The carrier mobilities were decreased in this experiment by repeatedly and sharply changing the sample temperature.

Figure 5 illustrates the changes in the form of the CVC with changing temperature. We see that an increase of the sample temperature leads to a decrease of the critical field E<sub>c</sub>, with a particularly fast decrease at T ≥ 12°K. With increasing temperature, the initial conductivity of the samples increases noticeably

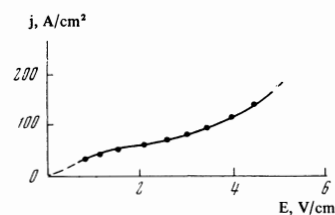


FIG. 3. CVC of sample No. 4 in weak electric fields.

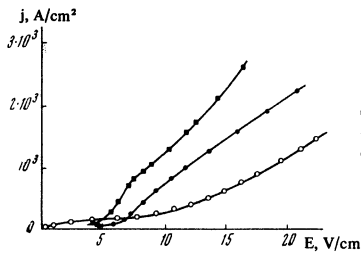


FIG. 4. Change in the shape of the CVC of sample No. 6 as a function of its quality ( $\delta = \rho(4.2^\circ\text{K})/\rho(300^\circ\text{K})$ ):  $\blacksquare$ — $\delta = 350$ ,  $\bullet$ — $\delta = 170$ ,  $\circ$ — $\delta = 100$ .

(as  $E \rightarrow 0$ ) and the kink in the CVC in fields  $\sim E_C$  becomes less and less pronounced. A negative differential resistance is retained approximately up to  $18^\circ\text{K}$ .

Figure 6 shows the dependence of the field  $E_C$  on the antimony concentration. In plotting this curve we used the values of  $E_C$  obtained for samples with the largest values of  $\delta$  and with current orientation along the binary axis. We see that  $E_C$  amounts to a fraction of a V/cm for samples with  $x \approx 0.07$ , but reaches  $\sim 14$  V/cm for samples with  $x \approx 0.17$ .

To determine the influence of carrier injection from the current contacts, and also of surface and size phenomena on the value of  $E_C$ , we investigated a series of samples cut from the same single-crystal ingot of  $\text{Bi}_{0.912}\text{Sb}_{0.088}$  and having different shapes (right parallelepipeds or dumbbells—Fig. 1), different cross-section areas (variation by a factor  $\sim 30$ ), different lengths (variation by a factor  $\sim 4$ ), and different positions of the potential contacts relative to the current contacts. No significant changes of  $E_C$  were observed in these experiments. Thus, the influence of injection from the current contacts and of surface and size phenomena on the value of  $E_C$  was not decisive in the performed experiments.

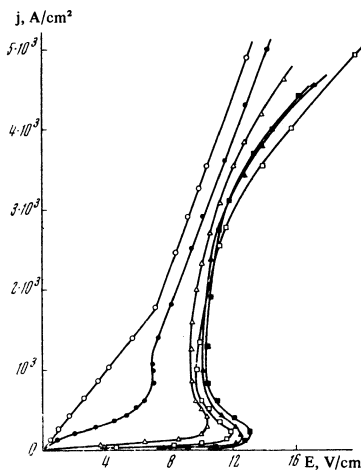


FIG. 5

FIG. 5 CVC of sample No. 2, measured at different temperatures:  $\blacksquare$ — $T = 2^\circ\text{K}$ ,  $\blacktriangle$ — $T = 4.2^\circ\text{K}$ ,  $\square$ — $T = 12.6^\circ\text{K}$ ,  $\triangle$ — $T = 14.3^\circ\text{K}$ ,  $\bullet$ — $T = 18^\circ\text{K}$ ,  $\circ$ — $T = 25^\circ\text{K}$ .

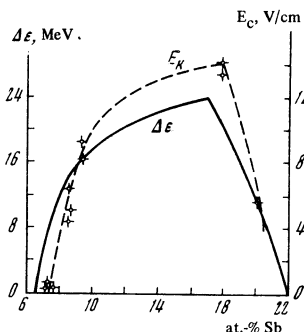


FIG. 6

FIG. 6. Dependence of the minimum energy gap  $\Delta\epsilon$  in the alloy  $\text{Bi}_{1-x}\text{Sb}_x$  (see Fig. 1 in [1]) and of the breakdown field  $E_C$  on the Sb concentration. Points—experimental values of the field  $E_C$  of samples 1, 2, 6, 15, and 17–23.

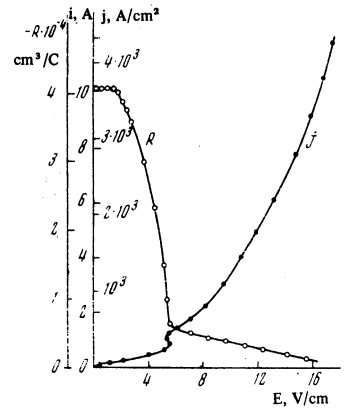


FIG. 7. Dependence of the Hall coefficient  $R$  on  $E$  and the CVC of sample No. 4:  $n_0 \approx 3 \times 10^{14} \text{ cm}^{-3}$ ,  $\mu \approx 3 \times 10^6 \text{ cm}^2/\text{V}\cdot\text{sec}$ .

Figure 7 shows the results of measurements of the Hall coefficient of an n-type  $\text{Bi}_{0.912}\text{Sb}_{0.088}$  sample. The absolute value  $|R|$  of the Hall coefficient decreased rapidly with increasing electric field intensity, and this effect sets in at electric field intensities much lower than  $E_C$ .

The CVC of most investigated samples of  $\text{Bi}_{0.912}\text{Sb}_{0.088}$  composition show, following a sharp increase of the current at  $E \geq E_C$ , a noticeable slowing down of the rate of this increase (Fig. 8). To explain this phenomenon we investigated the influence of a longitudinal magnetic field on the shape of the CVC. At  $E < E_C$  the magnetic field leads to an increase of the resistance, and at  $E_C < E < E'$  to a decrease (Fig. 8). At a fixed value of the longitudinal magnetic field, the negative magneto-resistance which occurs at  $E > E_C$  exists in a limited current region and disappears at  $E > E'$ . The higher the intensity of the longitudinal field, the larger the current at which the negative longitudinal magneto-resistance vanishes.

The transverse magnetoresistance was positive in the entire investigated range of electric and magnetic fields.

DISCUSSION OF RESULTS

The most probable cause of the sharp increase of the conductivity of the investigated samples in electric fields at  $E \approx E_C$  is, in our opinion, interband breakdown. This assumption is confirmed by the correlation of the field  $E_C$  corresponding to the start of the sharp increase of the conductivity with the width of the forbidden band in semiconducting  $\text{Bi}_{1-x}\text{Sb}_x$  alloys (Fig. 6).

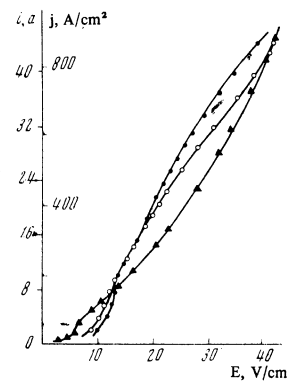


FIG. 8. CVC in longitudinal magnetic field (sample No. 10):  $\blacktriangle$ — $H = 0$ ,  $\circ$ — $H = 55 \text{ Oe}$ ,  $\bullet$ — $H = 100 \text{ Oe}$ .

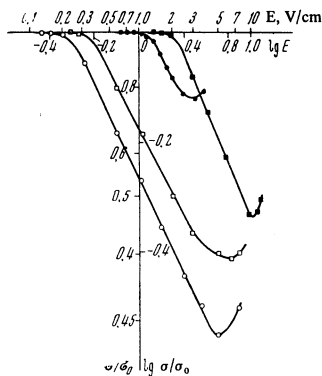


FIG. 9. Dependence of the conductivity  $\sigma/\sigma_0$  on the electric field  $E$  in the pre-breakdown region of electric fields:  $\circ$ —sample No. 16,  $\bullet$ —sample No. 4,  $\square$ —sample No. 3,  $\blacksquare$ —sample No. 17.

The absence of any noticeable dependence of the field  $E_C$  on the dimensions and shape of the sample, and also on the location of the potential contacts relative to the current contacts, indicates that the effect has a volume character and agrees with the assumption that interband breakdown takes place. The increase of the field  $E_C$  upon deterioration of the sample quality can also be explained on the basis of this hypothesis, namely, when the quality of the single crystal deteriorates, the free path decreases and a stronger electric field is necessary to acquire the same ionization energy.

For n-type samples in the pre-breakdown region, where the electron concentration is constant, the observed decrease of the conductivity  $\sigma$  with increasing electric field intensity can be attributed to the decrease of the mobility  $\mu$  of the carriers. If we neglect the different contributions made to the electric conductivity by those electron groups whose mobilities can differ somewhat, then it can be assumed that  $\sigma/\sigma_0 = \mu/\mu_0$ , where  $\sigma_0$  and  $\mu_0$  are the conductivity and the mobility in the region where Ohm's law is satisfied. Figure 9 shows, in a logarithmic scale, plots of  $\sigma/\sigma_0$  against the field  $E$  for samples 3, 4, 16, and 17, which have different antimony concentrations and different orientations of the current relative to the crystallographic axes. In a certain electric-field interval at  $E < E_C$ , these plots are straight lines with slopes ranging from  $-0.4$  to  $-0.5$  cm/V. The resultant relation  $\mu \propto E^{-0.4-0.5}$  is characteristic of scattering of hot electrons by acoustic phonons<sup>[8]</sup> in the approximation where the dispersion is quadratic.

Neglecting the singularities of the energy spectrum of the  $\text{Bi}_{1-x}\text{Sb}_x$  alloys, we can roughly estimate the electron temperature  $T_e$  by using the Shockley formula<sup>[9]</sup>, obtained assuming scattering by acoustic phonons:

$$\frac{T_e}{T} = \frac{1}{2} \left[ 1 + \left\{ 1 + \frac{3\pi}{8} \left( \frac{\mu_0 E}{u} \right)^2 \right\}^{1/2} \right].$$

For sample No. 4 at  $E = 2.5$  V/cm,  $\mu_0 = 3 \times 10^6$  cm<sup>2</sup>/V-sec,  $T = 4.2^\circ\text{K}$ , and a sound velocity  $u \approx 2 \times 10^5$ <sup>[10]</sup>, the electron temperature  $T_e$  turns out to be of the order of  $80^\circ\text{K}$ . Thus, it can apparently be assumed that the decrease of the mobility in the pre-breakdown region is connected with heating of the electrons by a strong electric field. With increasing field, a transition takes place from predominant scat-

tering by the ionized impurities in the region of weak electric fields<sup>[2]</sup> to predominant scattering by acoustic phonons. The predominant role of scattering by ionized impurities in weak electric fields is confirmed also by preliminary results of measurements of the conductivity in this field region. Following the initial ohmic section, a weak increase (by  $\sim 10$ – $20\%$ ) of the conductivity is observed, connected with the decrease of the effective cross section for scattering by ionized impurities with increasing electron energy.

The assumption that the scattering mechanism is altered makes it possible also to attribute the observed decrease of the Hall coefficient  $R = A/enc$  to a change in the value of  $A$  ( $A = 1.93$  for scattering by ionized impurities and  $A = 1.17$  for scattering by acoustic phonons).

We note that the decrease of mobility due to the current's own magnetic field in the pre-breakdown region does not exceed several percent.

The much faster than linear increase of the conductivity on Fig. 9 is connected with the increase of the carrier density at  $E \approx E_C$ .

The most perfect samples (Nos. 1–5) have reproducible S-shaped CVC under interband-breakdown conditions. Deterioration of sample quality leads to vanishing of the CVC section with negative differential resistance.

Unfortunately, we did not succeed in establishing uniquely the conditions for the occurrence on the CVC of a section with negative differential resistance. It is therefore still difficult to assess the physical cause of this phenomenon. One of the possible causes for the occurrence of a S-shaped CVC under conditions of interband breakdown may be the decrease of the scattering efficiency with increasing carrier density, owing to the increase of the screening of the scattering potentials in analogy with the situation obtaining in the mechanism proposed by Grandall<sup>[11]</sup> for the case of impact ionization of impurities in a compensated semiconductor.

The character of the CVC in the post-breakdown region can be attributed to the occurrence of a pinch effect in an electron-hole plasma produced as a result of interband breakdown, i.e., the compression of the carriers towards the sample axis under the influence of the self-magnetic field. The decrease of the current-column diameter as a result of the pinch effect leads to an increase of the magnetoresistance, owing to the increase of the self-magnetic field of the current. In addition, the strong growth of the carrier density on the sample axis causes an increase in the electron-hole scattering<sup>[12]</sup>. This results in a certain decrease of the differential conductivity upon occurrence of the pinch effect (Fig. 8, curve for  $H = 0$ ).

In the present investigation we diagnosed the pinch by the longitudinal-magnetic-field method<sup>[13]</sup>. The gist of this method is that when a longitudinal field of sufficient magnitude is applied, the pinch disintegrates and the conductivity of the sample increases, i.e., a negative longitudinal magnetoresistance appears. After disintegration of the pinch by the longitudinal magnetic field, further increase of the current through the sam-

ple should again lead to a pinching of the currents and the CVC measured in a magnetic field should come closer to those measured without the field, as is indeed observed in the experiments (Fig. 8).

The occurrence of the pinch effect should not depend on the transverse dimensions of the sample<sup>[13]</sup>; this is in good agreement with the obtained data.

The temperature possessed by the carrier gas under conditions when the pinch occurs can be roughly estimated from Bennett's relation<sup>[14]</sup>

$$I_c = 1.7 \cdot 10^5 T / v_{||}$$

where  $I_c$  is the critical current of pinch formation,  $v_{||} = v_e + v_h$  is the sum of the drift velocities of the electrons and holes, and  $T = T_e + T_h$  is the sum of the temperatures of the electron and hole gases.

For sample No. 4 we have  $I_c \approx 2$  A and the corresponding value of the field is  $E \approx 8$  V/cm. Assuming the hole and electron velocities to be the same,  $v_e \approx v_h \approx 10^7$  cm/sec (we have assumed here that the mobility of the electrons in fields corresponding to the occurrence of interband breakdown changes, as in pre-breakdown fields, in proportion to  $E^{-0.5}$ ), and assuming the electron and hole temperatures to be equal, we obtain from Bennett's relation  $T_e \approx T_h \approx 60^\circ\text{K}$ . The average carrier energy at such a temperature is  $kT_e \approx 5$  meV, i.e., it is approximately 0.3 of the forbidden band width ( $\Delta\epsilon \approx 15$  meV for sample No. 4), which is perfectly reasonable, recognizing the clearly approximate character of the estimate. We note also that estimates of the carrier temperature made by Glicksman<sup>[12]</sup> for InSb under analogous conditions (interband breakdown and pinch effect) give a value  $kT_e/\Delta\epsilon \approx 0.6$ , which agrees with our results.

In conclusion, we take the opportunity to express our sincere gratitude to Sh. M. Kogan, A. F. Volkov, and A. Ya. Shul'man for valuable critical remarks,

and also to G. A. Ivanov for supplying the high-grade  $\text{Bi}_{1-x}\text{Sb}_x$  single crystals.

<sup>1</sup>N. B. Brandt, S. M. Chudinov, and V. G. Karavaev, Zh. Eksp. Teor. Fiz. 61, 689 (1971) [Sov. Phys.-JETP 34, 000 (1972)].

<sup>2</sup>N. B. Brandt, Ya. G. Ponomarev, and Kh. Dittmann, Fiz. Tverd. Tela [Sov. Phys.-Solid State] (in press).

<sup>3</sup>G. A. Antcliffe, Phys. Lett., 27A, 606 (1968).

<sup>4</sup>N. B. Brandt, E. A. Svistov, E. A. Svistova, and V. Yu. Galkin, ZhETF Pis. Red. 10, 521 (1969) [JETP Lett. 10, 332 (1969)].

<sup>5</sup>N. B. Brandt, Pribory i Tekh. Eksperim. No. 2, 138 (1956).

<sup>6</sup>N. B. Brandt, E. A. Svistova, and R. G. Valeev, Zh. Eksp. Teor. Fiz. 55, 469 (1968) [Sov. Phys.-JETP 28, 245 (1969)].

<sup>7</sup>N. B. Brandt, E. A. Svistova, and M. V. Semenov, Pribory i Tekh. Eksperim. No. 2, 240 (1970).

<sup>8</sup>E. M. Conwell, Transport Properties, Suppl. 9 of Solid State Physics, ed. by F. Seitz and D. Turnbull.

<sup>9</sup>R. A. Smith, Semiconductors, Cambridge Univ. Press.

<sup>10</sup>Y. Eckstein, A. W. Lawson, and V. H. Rencker, J. Appl. Phys., 31, 150 (1960).

<sup>11</sup>A. Grandall, Phys. Chem. Sol., 31, 2069 (1970).

<sup>12</sup>M. Glicksman and M. C. Steele, Phys. Rev. Lett., 2, 461 (1959).

<sup>13</sup>A. G. Chynoweth and A. A. Murray, Phys. Rev., 123, 515 (1961).

<sup>14</sup>B. Ancker-Johnson, Plasmas in Semiconductors and Semimetals, Vol. 1, ed. by Willardson, N. Y., 1965, p. 434.

Translated by J. G. Adashko